J Mater Sci: Mater Med (2007) 18:1529–1536
DOI 10.1007/s10856-006-0115-9

Low-temperature deposition of rutile film on biomaterials substrates and its ability to induce apatite deposition in vitro

Jin-Ming Wu · Jin-Fang Liu · Satoshi Hayakawa · Kanji Tsuru · Akiyoshi Osaka

Received: 17 May 2005 / Accepted: 3 March 2006 / Published online: 5 April 2007

Abstract Low-temperature deposition of crystalline titania films on intrinsically bioinert materials to induce the bioactivity is of practical interest, not only because it meets the demand of providing organic biomaterials with bioactivity, which cannot tolerate high-temperature thermal treatments, but also because it reserves abundant Ti–OH groups facilitating the apatite deposition. In this paper, rutile films with thickness varied from 0.1 μm to 1.7 μm were deposited on commercially available pure titanium substrates from 1.5 M titanium tetrachloride aqueous solution kept at 60 °C for 3–60 h. The rutile films grew to give a preferred (101) crystalline plane in the X-ray diffraction pattern. After soaking in a simulated body fluid of the Kokubo solution (SBF) for 2 days, the rutile films with thickness over 0.6 μm were covered with a layer of apatite. All the films with various thickness induced apatite deposition in SBF after soaking for 5 days. The bioinert polytetrafluoroethylene (PTFE) was also found to exhibit remarkable in vitro bioactivity as to induce apatite deposition from SBF within 2 days, after depositing the rutile film on the surface.

This work is supported partly by the Natural Science Foundation of Zhejiang Province under the project No. M503011.

J.-M. Wu (✉) · J.-F. Liu
Department of Materials Science and Engineering, Zhejiang University, Hangzhou 310027, P. R. China
e-mail: msewjm@zju.edu.cn

S. Hayakawa · K. Tsuru · A. Osaka
Faculty of Engineering, Okayama University, Tsushima, Okayama-shi 700-8530, Japan

K. Tsuru · A. Osaka
Research Center for Biomedical Engineering, Okayama University, Tsushima, Okayama-shi 700-8530, Japan

Introduction

Various techniques have been developed to introduce a layer of titania on the surface of widely used commercially pure titanium (CPTi) to provide it with bioactivity, that is, the ability to bond directly and reliably to living bone in a shorter period after they are implanted in vivo [1–16]. The ability of the titania film to induce in vitro apatite deposition in the Kokubo's simulated body fluid (SBF, a metastable calcium phosphate solution similar in inorganic ion composition to human blood plasma, and is commonly used to evaluate the in vivo bioactivity) has been ascribed to both the Ti–OH functional groups and the negatively charged surface [9]. The importance to achieve a crystallized titania has also been stressed because amorphous titania exhibited very poor in vitro bioactivity [12]. A subsequent high-temperature thermal treatment is commonly required to induce the crystallization of the titania film, which reduces surely the Ti–OH groups facilitating the in vitro apatite deposition [1–8, 13–15]. Some attempts have been made to introduce crystalline titania film on the CPTi surface, without a subsequent thermal treatment, to obtain excellent bioactivity [12, 14–17]. For example, Wu et al. obtained crystalline titania film on the CPTi surface under a low temperature of 80 °C, which induced apatite deposition in SBF within 12 h [12, 14]. Xiao et al. reported that the bioactive crystalline titania film can also be derived through soaking CPTi in an oxysulfate solution at a low temperature of 60 °C [17]. Various crystallization routes such as laser treatment [15], ultraviolet irradiation and

water vapor exposure [16] have been utilized instead of thermal treatments to induce crystallization of sol-gel derived titania films.

To obtain bioactive crystalline titania films without such subsequent thermal treatment is of interest also because of their applicability to introducing bioactivity on organic substrates. Natural bone is a complicated composite with apatite nanocrystals depositing on three-dimensional structural organic collagen fibers [18, 19]. Efforts have been made to prepare bone substitutes with an analogous structure to that of natural bone through a biomimetic approach, the prerequisite of which is to provide organic biomaterials with the in vitro apatite deposition ability [20–24]. In addition, to induce bioactivity on organic biomaterials is also of practical use for them to be used as soft tissue substitutes such as ligaments, which should be brought into close contact with bone in some parts [25].

Apatite coating on organic substrates has been obtained through a few techniques, in which the key step is soaking relevant materials in 1.5 SBF, a solution with inorganic ion concentrations 1.5 times the SBF. In those cases, it is inevitable to introduce previously a functional layer of either calcium phosphate by bringing the organics in contact with a bioglass in SBF [20] or Si–OH groups by sol–gel coating [21] and vapor-phase photografting [22]. Yamaguchi et al. obtained the calcium phosphate layer on the surface of a soft tendon tissue through alternative soaking in a $CaCl_2$ and a Na_2HPO_4 solution [25]. Carbonxyl groups were also introduced on the surface of a chitin non-woven fabric [23] and gels of chitin and gellan gum [24]. After immersing into a saturated $Ca(OH)_2$ aqueous solution under nitrogen atmosphere, apatite began to precipitate on the surface after soaking in SBF. Apatite deposition was also obtained on highly porous PTFE membranes after soaking in SBF, through introducing a monolayer of monoacryloxyethyl phosphate onto the surface [19]. An electroless plating technique has been used to coat hydroxyapatite layer on the polymer substrates of high molecular weight polyethylene (HMWPE), starch/ethylene vinyl alcohol blends (SEVA) and starch/cellulose acetate blends (SCA), to provide them with in vitro bioactivities [26]. Kamitakahara et al. precipitated anatase on silicon substrates, through a series of procedures of soaking in tetraisopropyltitanate (TIPT) and then water, a hydrochloride solution, and then an ammonia solution or hot water. The amount of the deposited apatite in SBF increased with increasing amount of the precipitated anatase [27].

Most of the above-mentioned approaches either need careful control of preparation conditions such as dealing with the highly unstable 1.5 SBF [20–22], or involve multiplicate processes [27]. Wu et al. have developed a simple technique to provide various metallic biomaterials with bioactivity, through low-temperature deposition of anatase thin films on substrates from a titanium tetrafluoride solution. Unfortunately, the fluorine incorporated in the anatase film was found to inhibit the apatite deposition and hence a subsequent thermal treatment at temperatures beyond 300 °C was required to remove such adverse fluorine [10, 11]. In this study, tetrachloride was used instead of tetrafluoride, considering that SBF contains already significant amounts of chlorine ions and hence the possible incorporation of chlorine in the titania film should not disturb the apatite deposition.

Experimental procedure

Appropriate amount of ice was added to reagent grade $TiCl_4$ with purity of 99.0% (Kanto Chemical Co. Ltd., Japan) held in a beaker on an ice bath to prepare the $TiCl_4$ solution with a concentration of 1.5 M. The prepared solution was transparent and stable under the ambient environment for up to several months. Pieces of CPTi with a size of $10 \times 10 \times 1$ mm^3 were firstly treated at 60 °C for 2 min with a 1:1 (in volume) mixture of 5.50 M HF and 7.88 M HNO_3 solution, and then ultrasonically rinsed with distilled water for 5 min, three times. Pieces of polytetrafluoroethylene (PTFE) with a size of $10 \times 10 \times 1$ mm^3 were firstly treated with dilute nitric acid, and then ultrasonically rinsed with ethanol and distilled water. Three pieces of the samples were soaked in 10 mL of the $TiCl_4$ solution held in a polyethylene bottle (25 mm in diameter) with a tight screw cap and kept in an oven at 60 °C for up to 60 h. After soaking, the samples were rinsed gently with distilled water.

The in vitro bioactivity of the titania film was evaluated with SBF, which was prepared as described in Ref. [8], and pH adjusted to 7.4 at 36.5 °C with tris(hydroxymethylaminomethane) and hydrochloric acid. The samples were soaked in SBF at 36.5 °C for up to 10 d (15 mL for each piece).

Surface analysis was conducted with a thin-film X-ray diffractometry (XRD, RAD IIA, Rigaku, Japan), a Fourier transform infrared reflection spectroscopy (FT-IR, JASCO FT-IR300, Japan), an optical microscopy (KH-2700, HiRox Company, Ltd, Japan), a scanning electron microscopy (SEM, JEOL JSM-6300, Japan) with attached energy-dispersive X-ray spectroscopy (EDS). The film thickness was determined by the interference pattern of the reflection spectra collected using an UV–visible spectrophotometer (UV-2550, Shimadzu, Japan).

Results

Fig. 1 shows photograph of CPTi soaked in the $TiCl_4$ solution at 60 °C for different time. The color change due

to the interference of the reflected light from the oxide film, the thickness of which increases with prolonged soaking time, can be clearly seen. The average film thickness, obtained from three samples, is given in Fig. 2 as a function of the soaking time. The film thickness increased almost lineally with soaking time before 24 h, and then increased steadily to a value of 1. 7 μm after 60 h soaking in the $TiCl_4$ solution.

Figure 3 shows the TF-XRD patterns of the CPTi samples soaked in the $TiCl_4$ solution at 60 °C for 24 h. Broad peaks corresponding to rutile can be identified. A rough estimation of the crystallite size through the Scherrer formula [12], utilizing the more symmetrical (101) peak gave a value of ca. 10 nm. Therefore, rutile films with nanosized crystallites have been deposited directly under the low temperature environment. The intensity ratio of peaks corresponding to (101) and (110) crystalline planes or rutile was near 1, compared to 0.41 from the standard data (JCPDS 21-1276), suggesting an oriented growth of rutile.

Figure 4 shows the FT-IR spectra of CPTi after soaking in the $TiCl_4$ solution for various durations, followed by soaking in SBF for 2 d. The rutile phase gave a band located at 830 cm^{-1}. Two bands at 595 cm^{-1} and 546 cm^{-1}

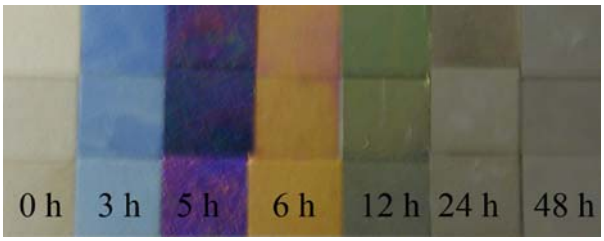

Fig. 1 Photograph of CPTi soaked in the $TiCl_4$ solution at 60 °C for different time, showing color changes due to the interference of the reflected light from the titania films with various thickness

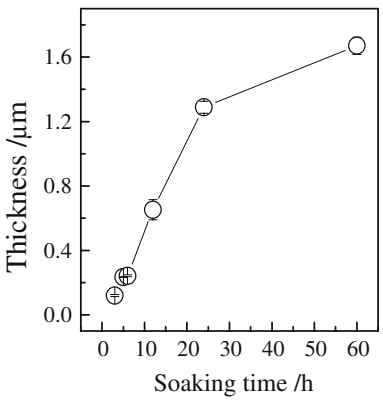

Fig. 2 Film thickness as a function of the soaking time in the $TiCl_4$ solution kept at 60 °C. The error bar was given by the standard deviation of three samples

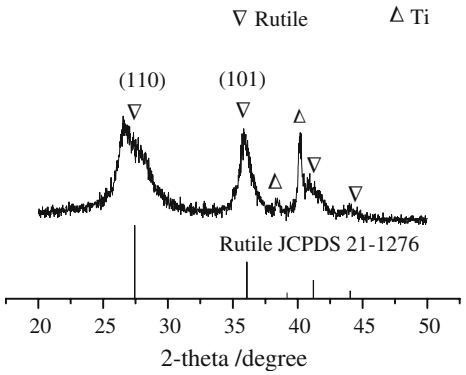

Fig. 3 TF-XRD patterns of CPTi soaked in the $TiCl_4$ solution at 60 °C for 24 h. Note the abnormal strong (101) plane of rutile

result from the v_4 mode of O–P–O bending in apatite, whereas the peaks at 1,108 cm^{-1} and 1,010 cm^{-1} indicate the v_3 band of P–O stretching mode. The peak at 472 cm^{-1} is ascribed to v_2 mode of O–P–O bending in apatite. The shoulder at 961 cm^{-1} reflects v_1 band of P–O stretching mode in apatite. The band at 875 cm^{-1} and the bands between 1,418 cm^{-1} and 1456 cm^{-1} corresponds to the carbonate incorporated in the apatite [8, 12, 28]. Therefore, after 2 d soaking in SBF, deposition of apatite incorporated with carbonate ions was evident on CPTi surfaces soaked in the $TiCl_4$ solution for over 12 h, which resulted in a film thickness beyond 0.6 μm.

Figure 5 illustrates the TF-XRD patterns of CPTi after soaking in the $TiCl_4$ solution for different time, followed by soaking in SBF for 2 d. Soaking CPTi in the $TiCl_4$ solution for 3 h and 6 h gave only the peak corresponding

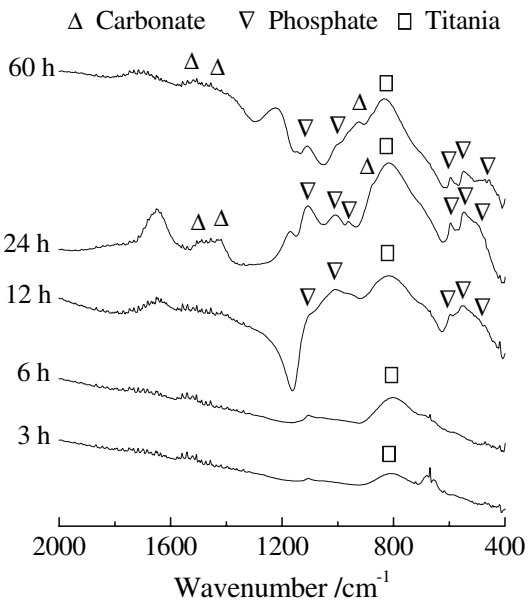

Fig. 4 FT-IR spectra of CPTi soaked in the $TiCl_4$ solution at 60 °C for different time, followed by soaking in SBF for 2 d

to (101) plane of rutile, due to its oriented growth. With increasing soaking time in the $TiCl_4$ solution, the (101) intensity increased and the peak corresponding to the (110) plane of rutile appeared, because of the increasing thickness of the rutile film. It is clear that the rutile film tended to grow preferably along the (101) plane, from the very beginning of the deposition procedure. After soaking in SBF for 2 d, for the samples with rutile film thickness exceeding a value of 0.6 μm, an extremely strong (002) peak corresponding to apatite can be discerned, suggesting a preferential growth of the apatite crystal. In addition, it can be seen that the XRD peaks corresponding to (211), (112) and (300) planes of apatite overlap to give a broad diffraction located around $2\theta = 32$ °, suggesting the deposition of poorly crystallized apatite [12, 28].

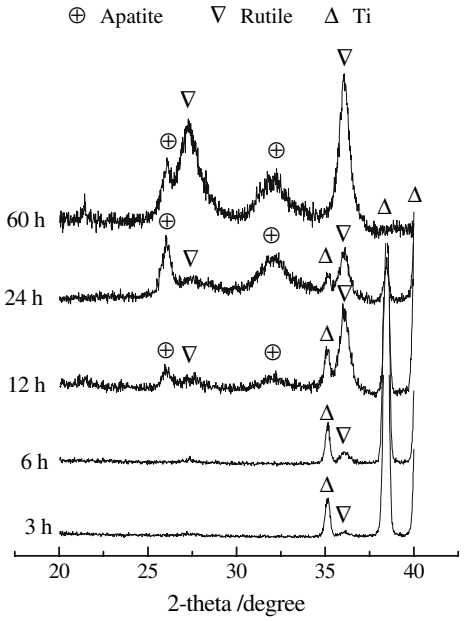

Fig. 5 TF-XRD patterns of CPTi soaked in the $TiCl_4$ solution at 60 °C for different time, followed by soaking in SBF for 2 d

Figure 6 shows colorful optical microscope images of CPTi soaked in the $TiCl_4$ solution at 60 °C for different time followed by soaking in SBF for 2 d. Titanium grains after pickling can be clearly seen for the samples soaked in the $TiCl_4$ solution for 3 h and 6 h. No apatite particles were observed on the two samples with relatively thinner rutile films after 2 d soaking in SBF. However, homogeneous apatite layer with cracks is evident on the samples soaked in the $TiCl_4$ solution for 12 h and 24 h, agreeing well with the FT-IR (Fig. 4) and TF-XRD (Fig. 5) results.

Figures 7 and 8 indicate TF-XRD patterns of CPTi soaked in the $TiCl_4$ solution at 60 °C for 3 h and 24 h, respectively, followed by soaking in SBF at 36.5 °C for various durations. Apatite deposition was evident on CPTi soaked in the $TiCl_4$ solution for 3 h only after 5 d soaking in SBF; however, for CPTi soaked in the $TiCl_4$ solution for 24 h, 2 d soaking in SBF was enough to give remarkable apatite layer on the surface. With the increasing soaking time in SBF, the intensity of the peaks corresponding to apatite increased and that of the peaks coming from CTTi and rutile decreased in both Figs. 7 and 8, suggesting the increased amounts of the precipitated apatite.

Table 1 lists the EDS results of CPTi soaked in the $TiCl_4$ solution at 60 °C for 24 h followed by soaking in SBF for different time. Chlorine was detected in the as-coated rutile films. Large amounts of P and Ca appeared

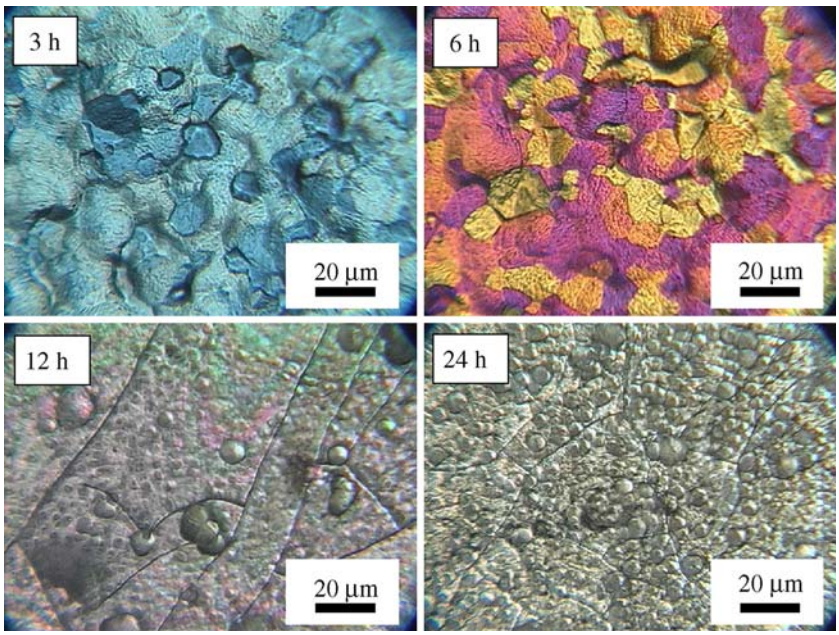

Fig. 6 Optical microscopy images of CPTi soaked in the $TiCl_4$ solution at 60 °C for different time, followed by soaking in SBF for 2 d

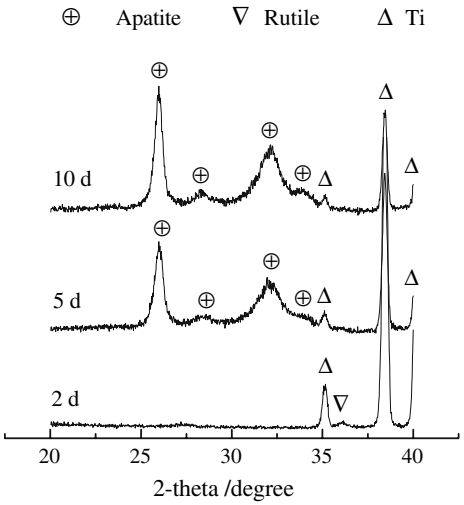

Fig. 7 TF-XRD patterns of CPTi soaked in the $TiCl_4$ solution at 60 °C for 3 h, followed by soaking in SBF for 2, 5 and 10 d

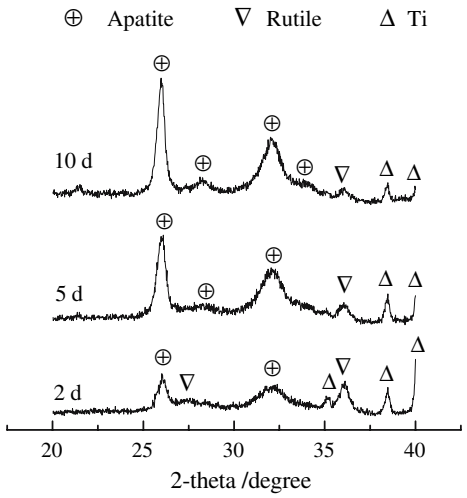

Fig. 8 TF-XRD patterns of CPTi soaked in the $TiCl_4$ solution at 60 °C for 24 h, followed by soaking in SBF for 2, 5 and 10 d

after soaking in SBF for a period longer than 2 d. The atomic ratio of Ca to P increased with increasing soaking time, with a value lower than 1.67, the stoichiometric hydroxylapatite.

Figures 9 and 10 illustrate FT-IR spectra and TF-XRD patterns, respectively, of PTFE soaked in the $TiCl_4$ solution at 60 °C for 48 h, and followed by soaking in SBF at 36.5 °C for various durations. The spectrum collected from the uncoated PTFE is also given as a reference. The results show that, rutile film has also been deposited on the PTFE substrates. Apatite deposition on the coated PTFE was evident after 2 d soaking in SBF.

The SEM morphology of the rutile-coated PTFE samples after soaking in SBF for 2, 5, and 10 d is shown in Fig. 11. Apatite globules with sizes of several micrometers are evident. Each globule is actually aggregates of numerous tiny flakes uniting together, which is the typical morphology of apatite precipitated from SBF [12, 28].

Table 1 Surface compositions of CPTi soaked in the $TiCl_4$ solution at 60 °C for 24 h followed by soaking in SBF for different time, obtained by EDS (at.%)

	O	Mg	Cl	P	Ca	Ti	Ca/P
As-coated	20.7	–	6.0	–	–	Bal.	–
SBF 2 d	33.7	2.1	0.1	14.2	19.2	Bal.	1.35
SBF 5 d	35.6	0.6	–	22.4	35.8	Bal.	1.60
SBF 10 d	34.2	2.8	–	22.4	37.1	Bal.	1.66

The EDS results of the PTFE substrates soaked in the $TiCl_4$ solution at 60 °C for 48 h followed by soaking in SBF for different time are listed in Table 2. The appearance of Ti strongly suggests the introduction of the titania layer on the surface after soaking in the $TiCl_4$ solution. Similar to the CPTi samples (Table 1), P and Ca, the ratio of which did not exceed that of the stoichiometric hydroxylapatite, were detected after 2 d soaking in SBF.

Discussion

The followed hydrolysis reaction took place immediately after adding water to $TiCl_4$ according to Kim et al. [29],

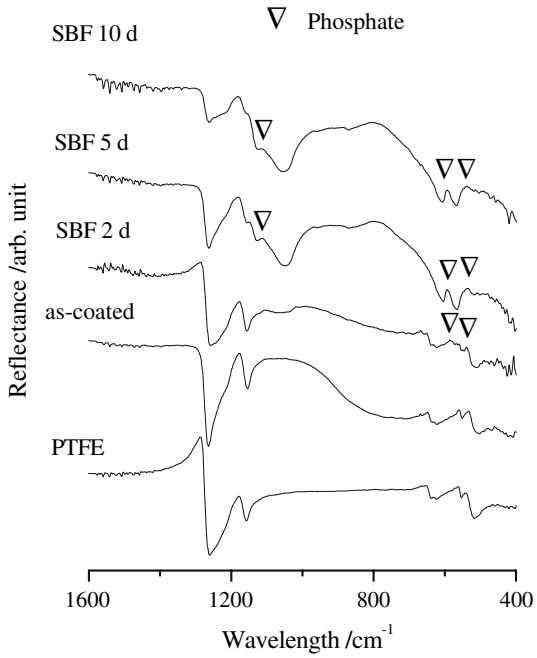

Fig. 9 FT-IR spectra of PTFE soaked in the $TiCl_4$ solution at 60 °C for 48 h, followed by soaking in SBF for 0, 2, 5 and 10 d. Peaks not identified came from the PTFE substrates

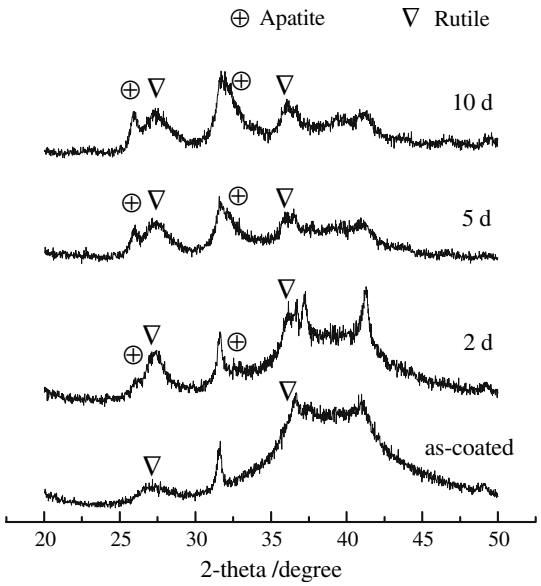

Fig. 10 TF-XRD patterns of PTFE coated with the rutile films through soaking in the $TiCl_4$ solution at 60 °C for 48 h, followed by soaking in SBF for 0, 2, 5 and 10 d. Peaks not identified came from the PTFE substrates

$$TiCl_4 + H_2O \rightarrow TiOCl_2 + 2HCl$$

Nanosized rutile powders can be obtained through homogeneous precipitation from the above solution with concentration of 0.5 M, which was kept at a temperature range between room temperature and 65 °C [29]. A mixture of anatase and rutile was obtained when keeping the solution at temperatures between 65 °C and 100 °C [29]. In the present work, as CPTi or PTFE was soaked in the 1.5 M $TiCl_4$ solution for a longer period, the rutile films precipitated from the solution heterogeneously on the CPTi and PTFE substrates and on the bottom and wall of the polyethylene bottle, too. No homogeneous precipitation of titania powders was observed before ca. 24 h of soaking at 60 °C. The film thickness increased gradually with soaking time. The deposited rutile films grew preferably along the (101) crystalline plane, from the very beginning of the soaking procedure. It is noted that the oriented growth of rutile is a common phenomena when it is precipitated through heterogeneous nucleation from various solutions [30–32].

The low-temperature deposited rutile films with thickness exceeding 0.6 μm possessed excellent in vitro bioactivity as inducing thorough apatite coverage on surface in SBF within 2 d. Such apatite-forming ability is significantly better than those thermally derived crystalline titania layers [2–4, 7–9], and comparable to the low-temperature crystallized one [12]. Among the three polymorphs of titania, that is, anatase, rutile and brookite, the bioactivity of anatase is the most studied. The apatite deposition has been found to be more pronounced on the anatase gel than on the rutile gel, both of which are prepared by a sol-gel process followed by heating under different temperatures [13]. Titania coating derived by soaking in an anatase slurry is also found to induce more apatite deposition than that derived by soaking in a rutile slurry [33]. However, Wu et al. already pointed out that the low-temperature prepared titania film consisted predominantly of rutile is effective to the same extent as that consisted of pure

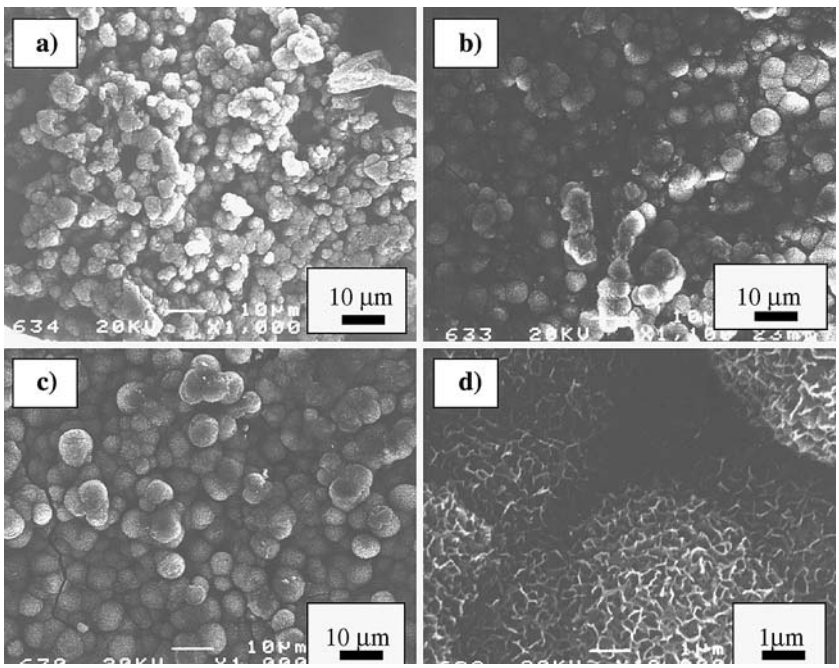

Fig. 11 SEM morphologies of the rutile-coated PTFE after soaking in SBF for (**a**) 2 d, (**b**) 5 d, (**c**) and (**d**) 10 d

Table 2 Surface composition of rutile-coated PTFE after soaking in SBF for different time, obtained by EDS analysis (at.%)

	O	Mg	Cl	P	Ca	Ti	Ca/P
As-coated	Bal.	–	1.8	–	–	25.5	–
SBF 2 d	Bal.	2.1	0.4	12.2	20.3	30.1	1.66
SBF 5 d	Bal.	2.8	3.8	15.8	22.7	20.4	1.44
SBF 10 d	Bal.	1.8	0.5	19.0	29.7	14.9	1.56

anatase in inducing apatite deposition in SBF [12]. It is noted that the pure rutile films derived by various chemical and electrochemical methods have been reported recently to exhibit high ability to induce apatite deposition in SBF [2, 7, 15, 34]. Therefore, it can be concluded now that the rutile phase possesses higher, or at least the same, ability to induce apatite deposition in SBF, in case that the rutile film contains Ti–OH functional groups.

The early apatite deposition ability was slightly reduced with decreasing film thickness, agreeing with the results obtained by Wang et al. [3]. Peltola et al. also reported that increasing the number of coating layers for the sol–gel derived titania on CPTi also enhanced the apatite-forming ability, which was attributed to the increased specific surface area as well as pore volume and pore size [8]. Fluorine atoms incorporated in the titania layer inhibited apatite deposition [10, 11]. Although significant amount of chlorine atoms were found incorporating in the rutile films (Table 1), the films also induced apatite deposition effectively. This is not strange since the SBF used to assess the in vitro bioactivity already includes 147.8 mM chlorine ions, which should have not disturbed the apatite deposition.

The present experiment shows that rutile films with excellent in vitro bioactivity can be obtained at a low temperature of 60 °C. The rutile film with nanosized crystallites induced effectively apatite deposition in SBF, without the necessity of any post-treatments. Since this aqueous approach can be easily applied to various substrates with complicated shape, the present method provided a versatile method to induce bioactivity on various biomaterials.

Conclusion

Rutile films with excellent in vitro bioactivity were deposited on titanium and PTFE substrates at a low temperature of 60 °C. Chlorine atoms in the rutile films did not inhibit the apatite deposition in SBF. It is proved that rutile, just like anatase, also promotes apatite deposition. The present experiment provided a simple and versatile method to induce bioactivity on various biomaterials.

References

1. S. KANEKO, K. TSURU, S. HAYAKAWA, S. TAKEMOTO, C. OHTSUKI, T. OZAKI, H. INOUE and A. OSAKA, *Biomaterials* **22** (2001) 875
2. Y. X. LIU, K. TSURU, S. HAYAKAWA and A. OSAKA, *J. Ceram. Soc. Jpn.* **112** (2004) 452
3. X. X. WANG, S. HAYAKAWA, K. TSURU and A. OSAKA, *Biomaterials* **23** (2002) 1353
4. C. X. WANG, M. WANG and X. ZHOU, *Biomaterils* **24** (2003) 3069
5. W. H. SONG, Y. K. JUN, Y. HAN and S. H. HONG, *Biomaterials* **25** (2004) 3341
6. S. FUJIBAYASHI, T. NAKAMURA, S. NISHIGUCHI, J. TAMURA, M. UCHIDA, H. H. KIM and T. KOKUBO, *J. Biomed. Mater. Res.* **56** (2001) 562
7. H. M. KIM, F. MIYAJI, T. KOKUBO, S. NISHIGUCHI and T. NAKAMURA, *J. Biomed. Mater. Res.* **45** (1999) 100
8. T. PELTOLA, M. PATSI, H. RAHIALA, I. KANGASNIEMI and A. YLI-URPO, *J. Biomed. Mater. Res.* **41** (1998) 504
9. P. J. LI, I. KANGASNIEMI, K. de GROOT and T. KOKUBO, *J. Am. Ceram. Soc.* 77 (1994) 1307
10. J. M. WU, S. HAYAKAWA, K. TSURU, A. OSAKA and X. X. WANG, *Thin Solid Films* **414** (2002) 275
11. J. M. WU, F. XIAO, H. SATOSHI, K. TSURU, S. TAKEMOTO and A. OSAKA, *J. Mater. Sci. Mater. Med.* **14** (2003) 1027
12. J. M. WU, S. HAYAKAWA, K. TSURU and A. OSAKA, *J. Am. Ceram. Soc.* **87** (2004) 1635
13. M. UCHIDA, H. M. KIM, T. KOKUBO, S. FUJIBAYASHI and T. NAKAMURA, *J. Biomed. Mater. Res.* **64A** (2003) 164
14. J. M. Wu, H. SATOSHI, K. TSURU and A. OSAKA, *J. Ceram. Soc. Jpn.* **110** (2002) 78
15. N. MORITZ, S. AREVA, J. WOLKE and T. PELTOLA, *Biomaterials* **26** (2005) 4460
16. H. IMAI, H. HIRASHIMA and K. AWAZU, *Thin solid films* **351** (1999) 91
17. F. XIAO, K. TSURU, S. HAYAKAWA and A. OSAKA, *Thin Solid Films* **441** (2003) 271
18. W. BONFIELD, An Introduction to bioceramics; edited by L. L. Hench and J. Wilson, World Scientific, Singapore, 1993, p. 299
19. L. GRØNDAHL, F. CARDONA, K. CHIEM, E. WENTRUP-BYRNE and T. BOSTROM, *J. Mater. Sci. Mater. Med.* **14** (2003) 503
20. M. TANAHASHI, T. YAO, T. KOKUBO, M. MINODA, T. MIYAMOTO, T. NAKAMURA and T. YAMAMURO, *J. Am. Ceram. Soc.* **77** (1994) 2805
21. A. OYANE, K. NAKANISHI, HYUN-MIN KIM, F. MIYAJI, T. KOKUBO, N. SOGA and T. NAKAMURA, *Biomaterials* **20** (1999) 79
22. H. M. KIM, M. UENOYAMA, T. KOKUBO, M. MINODA, T. MIYAMOTO and T. NAKAMURA, *Biomaterials* **22** (2001) 2489
23. T. KOKUBO, M. HANAKAWA, M. KAWASHITA, M. MINODA, T. BEPPU, T. MIYAMOTO and T. NAKAMURA, *Biomaterials* **25** (2004) 4485
24. M. KAWASHITA, M. NAKAO, M. MINODA, H. M. KIM, T. BEPPU, T. MIYAMOTO, T. KOKUBO and T. NAKAMURA, *Biomaterials* **24** (2003) 2477
25. I. YAMAGUCHI, T. KOGURE, M. SAKANE, S. TANAKA, A. OSAKA and J. TANAKA, *J. Mater. Sci. Mater. Med.* **14** (2003) 883
26. I. B. LEONOR and R. L. REIS, *J. Mater. Sci. Mater. Med.* **14** (2003) 435
27. M. KAMITAKAHARA, M. KAWASHITA, N. MIYATA, T. KOKUBO and T. NAKAMURA, *J. Ceram. Soc. Jpn.* **112** (2004) 594

28. P. J. LI, *J. Biomed. Mater. Res.* **66A** (2003) 79
29. S. J. KIM, S. D. PARK, Y. H. JEONG and S. PARK, *J. Am. Ceram. Soc.*, 82 (1999) 927
30. J. M. WU, *J. Cryst. Growth* **269** (2004) 347
31. E. HOSONO, S. FUJIHARA, K. KAKIUCHI and H. IMAI, *J. Am. Chem. Soc.* **126** (2004) 7790
32. S. YAMABI and H. IMAI, *Chem. Mater.* **14** (2002) 609
33. R. ROHANIZADEH, M. AL-SADEQ and R. Z. LEGEROS, *J. Biomed. Mater. Res.* **71A** (2004) 343
34. T. Y. XIONG, X. Y. CUI, H. M. KIM, M. KAWASHITA, T. KOKUBO, J. WU, H. Z. JIN and T. NAKAMURA, *Key. Eng. Mater.* **254–256** (2004) 375